The Astrophysical Journal, 692:L45–L49, 2009 February 10 doi:10.1088/0004-637X/692/1/L45

PARTICLE ACCELERATION BY STRONG TURBULENCE IN SOLAR FLARES: THEORY OF SPECTRUM EVOLUTION

A. M. Bykov[1] and G. D. Fleishman[1,2]
[1] Ioffe Institute for Physics and Technology, 194021 St. Petersburg, Russia
[2] New Jersey Institute of Technology, Newark, NJ 07102, USA
Received 2008 May 16; accepted 2008 December 29; published 2009 January 22

ABSTRACT

We propose a nonlinear self-consistent model of the turbulent nonresonant particle acceleration in solar flares. We simulate temporal evolution of the spectra of charged particles accelerated by strong long-wavelength MHD turbulence taking into account the back-reaction of the accelerated particles on the turbulence. The main finding is that the nonlinear coupling of accelerated particles with MHD turbulence results in prominent evolution of the spectra of accelerated particles, which can be either soft–hard–soft or soft–hard–harder depending on the particle injection efficiency. Such evolution patterns are widely observed in hard X-ray and gamma-ray emission from solar flares.

Key words: acceleration of particles – diffusion – shock waves – Sun: flares – Sun: X-rays, gamma rays – turbulence

A solar flare arises due to fast and spatially localized strong energy release and reveals itself in electromagnetic radiation and particle flows. Details of the energy release (as well as energy storage) are currently under debate. Models based on the idea of magnetic reconnection are the most popular at the moment (Shibata 1999), while interesting alternative possibilities, such as ballooning instability (Shibasaki 2001), or circuit models (Zaitsev & Stepanov 1992) are discussed as well.

A common feature of the solar flares (as well as other astrophysical objects with strong energy release) is the production of nonthermal accelerated particles. There is now ample evidence of particle acceleration in flares (Meyer et al. 1956; Mathews & Venkatesan 1990; Cane et al. 1986; Chupp 1990; Akimov et al. 1992). Accelerated electrons reveal themselves in a variety of nonthermal emissions observed from radio range to gamma rays. Even rather small numbers of accelerated electrons arising under a weak acceleration process can be visible when the electrons produce coherent radio emission (e.g., Benz 1986; Fleishman et al. 2002). Nonthermal incoherent emissions (gyrosynchrotron and/or bremsstrahlung) are detectable when the acceleration is strong enough, provided there is a considerable fraction of background electrons to be accelerated.

Observations made by *RHESSI* in recent years have provided us with new stringent constraints on the acceleration mechanism(s) operating in flares. Grigis & Benz (2004, 2005) investigated spectral evolution during individual subpeaks of the impulsive hard X-ray (HXR) emission and found each such subpeak to display a soft–hard–soft (SHS) evolution; the property, which was earlier established for the impulsive phase as a whole (Parks & Winckler 1969; Kane & Anderson 1970; Benz 1977; Brown & Loran 1985; Lin & Schwartz 1987). Grigis & Benz (2004, 2005) concluded accordingly that the ability to reproduce the SHS spectrum evolution of the accelerated particle population must be an intrinsic property of the acceleration mechanism involved; it is the observational property of the acceleration mechanism that is addressed in this Letter.

A number of acceleration mechanisms and models have been proposed to account for the particle acceleration in flares (see, for a review, Aschwanden 2002). Acceleration by DC electric fields, both sub-Dreicer and super-Dreicer, has been considered (Holman 1985; Tsuneta 1985; Holman & Benka 1992; Litvinenko 1996). This process is able to provide the energization of particles up to 100 keV; thus, it can be considered as a possible mechanism of pre-acceleration in flares.

Stochastic acceleration by turbulent waves is currently assumed to provide the main acceleration in impulsive solar flares (Miller et al. 1996; Miller 1997; Hamilton & Petrosian 1992; Petrosian et al. 1994; Park et al. 1997; Pryadko & Petrosian 1998), while classical diffusive shock acceleration is believed to play a role in large-scale gradual events. Miller et al. (1997) made a detailed comparison between various acceleration scenarios and concluded that stochastic acceleration is intrinsically consistent with the observational constraints on the acceleration time, highest particle energy, and the total number of accelerated particles. In this Letter, we demonstrate that turbulent stochastic acceleration is also naturally consistent with the SHS spectrum evolution of accelerated particles.

Grigis & Benz (2006) noticed that within the standard model of stochastic acceleration (Miller et al. 1996) the higher level of turbulence results in a harder steady-state spectrum of accelerated electrons and vice versa, which looks consistent with the observed SHS evolution. It is, nevertheless, unclear if the real evolution of the spectrum will represent the sequence of such steady-state spectra or will behave differently. We note, however, that a fraction of stronger events (typically, proton reach events) displays a different kind of spectral evolution, namely, soft–hard–harder (SHH; Frost & Dennis 1971; Cliver et al. 1986; Kiplinger 1995; Saldanha et al. 2008), as well as the gradual phase of the impulsive events (Grigis & Benz 2008); we return to this point later.

Another important point firmly established by *RHESSI* data analysis (Brown et al. 2007; Dennis et al. 2007; Hudson & Vilmer 2007) is that a significant fraction (some tens of percent) of the released energy goes into nonthermal accelerated particles. This conclusion is also confirmed by radio data. Bastian et al. (2007) performed a calorimetry of the accelerated electron energy in a solar flare. They analyzed the radio spectrum evolution of a dense flare, when most of the accelerated electron energy was deposited into the coronal loop (rather than into the chromosphere). This made it possible to accurately measure the total energy deposited by the accelerated electrons into the coronal thermal plasma, which turned out to be as high as 30% of the estimated magnetic energy of the flaring loop. These findings imply that the back-reaction of the acceleration particles on the

accelerating agent (e.g., the turbulence) is not negligible, in full agreement with time-dependent test particle analytical solutions (Bykov & Fleishman 1992) and numerical modeling (Cargill et al. 2006), so this back-reaction must be properly taken into account by the acceleration model.

As we have noticed, the stochastic acceleration of the charged particles is the most promising candidate for particle acceleration in flares (e.g., Miller et al. 1997; Grigis & Benz 2006). However, the aforementioned energetic requirements complicate strongly the whole theory of stochastic acceleration. First of all, the turbulence energy must be large enough to supply the accelerated particles with sufficient energy. This means that the turbulence is strong, so nonlinear effects are important (e.g., Yan et al. 2008) and the (quasilinear) approximation of the weak resonant wave–particle interaction is no longer valid. Therefore, the theory must include a more general transport equation valid in the case of strong large-scale turbulence. Second, since this turbulence loses a large fraction of its energy in accelerating particles, this damping rate must be properly taken into account; thus, one needs to solve two coupled equations—one for the particles and the other for the turbulence.

The renormalized theory of particle acceleration by strong turbulence was developed by Bykov & Toptygin (1990a, 1990b); see also the review by Bykov & Toptygin (1993). The form of the equation for the averaged distribution function of nonthermal particles depends on whether the turbulence is composed of smooth (wavelike) fluctuations only or contains also the shock fronts and other discontinuities (Bykov & Toptygin 1993). Observations of the magnetic field complexity in the flare-productive active regions (Abramenko 2005) along with various models of primary energy release in flares (Shibata 1999; Shibasaki 2001; Zaitsev & Stepanov 1992; Vlahos 2007) suggest many ways of producing long-wave MHD turbulence (e.g., Miller et al. 1997; Grigis & Benz 2006) including possibly a shock wave ensemble (Anastasiadis & Vlahos 1991). Although the generation of discontinuities is likely under the impulsive energy release (e.g., Vlahos 2007), we limit our consideration to the case of smooth long-wave turbulence only, but will include the effect of the shocks in a further study.

We therefore adopt the following scenario. The process of flare energy release is accompanied by the formation of large-scale flows and broad spectra of MHD fluctuations in a reasonably tenuous plasma with frozen-in magnetic fields. Vortex electric fields generated by the compressible component of the large-scale motions of highly conductive plasma will result in efficient *nonresonant* acceleration of charged particles.

The distribution function $N(\boldsymbol{r}, p, t)$ of nonthermal particles averaged over an ensemble of turbulent motions satisfies the kinetic equation

$$\frac{\partial N}{\partial t} - \frac{\partial}{\partial r_\alpha}\,\chi_{\alpha\beta}\,\frac{\partial N}{\partial r_\beta} = \frac{1}{p^2}\,\frac{\partial}{\partial p}\,p^4 D(t)\,\frac{\partial N}{\partial p} + F_i(p). \qquad (1)$$

The particle source term, $F_i(p)$, is determined by injection of the electrons and nuclei. Although we do not consider explicitly the injection process, we note that there are many ways to inject particles into the stochastic acceleration by strong turbulence. The possibilities are various versions of DC acceleration (Litvinenko 1996, 2000, 2003) or resonant stochastic acceleration by small-scale waves (Miller et al. 1997). A nice option proposed recently by Fletcher & Hudson (2008) is that the reconfiguration of the preflare magnetic field can result in large-scale pulses of Alfvén waves, which in the presence of strong spatial gradients will generate field-aligned electric regions capable of accelerating electrons from the thermal pool up to 10 keV or above. Our further analysis does not depend on the specific injection mechanism and details of the particle injection process. Then, the phase-space diffusion coefficients D and $\chi_{\alpha\beta} = \chi\,\delta_{\alpha\beta}$ are expressed in terms of the spectral functions that describe correlations between large-scale turbulent motions (see Bykov & Toptygin 1993). The kinetic coefficients satisfy the following renormalization equations:

$$\chi = \kappa + \frac{5}{2}\int \frac{d^3\mathbf{k}\,d\omega}{(2\pi)^4}\left[\frac{2T+S}{i\omega + k^2\chi} - \frac{2k^2\chi S}{\left(i\omega + k^2\chi\right)^2}\right], \qquad (2)$$

$$D = \frac{\chi}{9}\int \frac{d^3\mathbf{k}\,d\omega}{(2\pi)^4}\,\frac{k^4 S(k,\omega,t)}{\omega^2 + k^4\chi^2}, \qquad (3)$$

where $T(k,\omega,t)$ and $S(k,\omega,t)$ are, respectively, the transverse and longitudinal parts of the Fourier components of the turbulent velocity correlation tensor. The equations for $T(k,\omega,t)$ and $S(k,\omega,t)$ can be found in Bykov (2001). We reproduce here only the equation for the longitudinal spectral function $S(k,\omega,t)$ responsible for the particle acceleration:

$$\frac{\partial S(k,\omega,t)}{\partial t} - \frac{\partial \Pi^S_\alpha(k,\omega,t)}{\partial k_\alpha} = \gamma_{ST}T(k,\omega,t) - \gamma_{dS}S(k,\omega,t) - \gamma_{ap}S(k,\omega,t). \qquad (4)$$

This full equation includes the nonlinear cascading flux, $\Pi^S_\alpha(k,\omega,t)$, as well as coupling with the transverse function ($\gamma_{ST}T(k,\omega,t)$), the true damping ($-\gamma_{dS}S(k,\omega,t)$, and the damping due to the acceleration of the charged particles ($-\gamma_{ap}S(k,\omega,t)$). Although all corresponding processes are generally relevant for the turbulence evolution, we found that only the last of them is critically important for providing the SHS spectrum evolution due to nonlinear nonresonant particle acceleration by strong turbulence. In the case of a single-scale long-wavelength injection of turbulent motion (Gaussian spectrum with the characteristic wavenumber k_0) we can neglect both the cascading term on the left-hand side and the direct turbulence damping $\gamma_{dS} = 0$. The turbulence is assumed to be confined in the acceleration region; possible turbulence leakage from the acceleration region is compensated by the adopted sustained source of the transverse component of large-scale turbulence. Particles, however, can escape from the region through its boundaries because of the large mean free path of particles outside the region. We therefore consider a simplified equation for $S(k,\omega,t)$:

$$\frac{\partial S(k,\omega,t)}{\partial t} = \gamma_{ST}T(k,\omega,t) - \gamma_{ap}S(k,\omega,t), \qquad (5)$$

where the expression for the damping rate of large-scale turbulence due to particle acceleration is $\gamma_{ap} = \theta D$. The parameter θ was determined (iteratively) in such a way as to preserve conservation of the total energy in the system of the turbulence and the particles, taking account of energetic particle escape from the acceleration region. The standard Crank–Nikolson scheme, providing second-order accuracy in time evolution, was applied to integrate Equations (1)–(5). The spatial transport term in Equation (1) was approximated as (time-dependent) escape time $N/T_{\rm esc}$, where $T_{\rm esc} = R^2/4\chi$, with R being the characteristic size of the acceleration region. Actually, the temporal evolution of χ is very slow since in Equation (2) it is dominated by the transverse component of

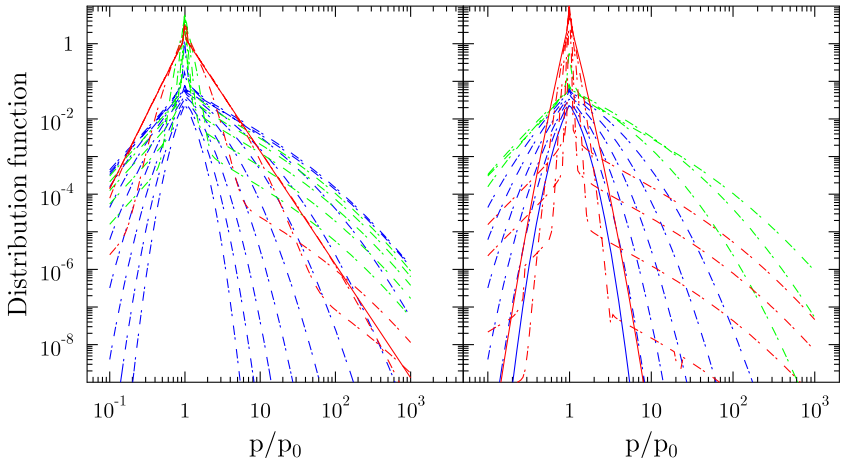

Figure 1. Temporal evolution of particle distribution function (sequence of $p^2\,N$ vs. p/p_0 plots, where p/p_0 is the dimensionless particle momentum normalized by the injection momentum p_0) simulated within a flare acceleration region of the scale size $R = 14\pi/k_0$ for the particle injection energy loading parameters $\zeta_i = 10^{-3}$ (left panel) and $\zeta_i = 0.1$ (right panel). Particle spectra are shown in 20 logarithmically distributed consequent time frames measured in $t\,D(0)$ starting from 0.01 to 30. For some typical parameters, e.g., $R = 2 \times 10^9$ cm, $B = 300$ G, $n = 10^9$–10^{11} cm^{-3}, we have $v_A \simeq 2.2 \times (10^8$–$10^9)$ cm s^{-1}, and the characteristic acceleration time $\tau_{\rm acc} \equiv 1/D(0) \simeq 1$–$10$ s in agreement with HXR (Grigis & Benz 2006) and radio (Bastian et al. 2007) observations.

the turbulence $T(k, \omega, t)$, which decays more slowly than the longitudinal component $S(k, \omega, t)$.

The temporal evolution of the turbulence is, thus, solely due to the particle acceleration effect. Particle acceleration time in the model is longer than the turnover time of large-scale MHD motions provided that $\omega > D$. Our simplified model assumes, therefore, that the turbulence is primarily produced in the form of transverse motions with a scale about $2\pi/k_0$ with a Gaussian spectrum, which produces the corresponding longitudinal turbulence due to the mode coupling ($\gamma_{ST}\,T(k, \omega, t)$) in a system of a finite scale size R (where $R\,k_0 > 1$). Furthermore, the model accounts only for the evolution of large-scale (energy-containing) motions of $k\,\lambda(p) \ll 1$, where $\lambda(p)$ is particle mean free path due to scattering by small-scale (resonant and nonresonant) magnetic field fluctuations; the corresponding diffusion coefficient is $\kappa = v\lambda(p)/3$. We did not consider here the turbulence cascade to resonant (small) scales (see Miller et al. 1996 Petrosian & Bykov 2008). Instead, we fixed the "microscopic" diffusion coefficient $\kappa(p)$ due to small-scale fluctuations, provided perhaps by the whistler waves, and considered the case of intensive large-scale turbulent motions provided $\kappa(p) < k_0^{-1} \cdot \sqrt{\langle u^2 \rangle}$. The kinetics of particles satisfying this inequality is determined by turbulent advection and so does not depend on the details of the "microscopic" diffusion coefficient.

The energy range, where this inequality holds, does depend on the charged particle mean free path $\lambda(p)$, which is ultimately defined by the generally unknown level of the small-scale turbulence. Bastian et al. (2007) determined the mean free path of the radio-emitting electrons (a few MeV) to be about 10^7 cm from the characteristic decay time of the radio light curves for the case when the turbulent transport of the particles was independently confirmed. This estimate is consistent with the small-scale (tens of cm) turbulence level of about $\sim 10^{-7}$ to 10^{-5} derived from a decimetric continuum burst analysis (Nita et al. 2005). Thus, to be conservative, in the case of electrons our approximation is firmly justified at least up to an energy of about 1 MeV, where the particle transport is fully driven by the large-scale turbulence and therefore it does not depend on the actual momentum dependence of the mean free path $\lambda(p)$. Then the model accounts for a nonlinear back-reaction of accelerated particles on large-scale motions only. Although the assumed presence of the small-scale turbulence implies the possibility of stochastic resonant acceleration along with nonresonant acceleration, considered here, we do not take into account the resonant acceleration explicitly, because the energy density of the small-scale turbulence is much smaller than that of the large-scale turbulence. As has been discussed, the resonant acceleration can, nevertheless, contribute to the injection term $F_i(p)$ in Equation (1).

We consider injection of nonrelativistic particles of momentum p_0, i.e. $F_i(p) \propto \delta(p - p_0)$. It is convenient to characterize the injection efficiency by the injection energy loading parameter

$$\zeta_i = \frac{2\int \epsilon(p) F_i(p) p^2 dp}{D(0)\,\rho\,\langle u^2 \rangle}, \qquad (6)$$

where $\epsilon(p)$ is the particle kinetic energy expressed via its momentum p. In Figure 1, we show the particle distribution function (normalized $\propto p^2 N$) calculated for the model. We assumed continuous injection of monoenergetic particles (electrons and protons $i = e, p$) with the injection energy loading parameters $\zeta_e = 10^{-3}$ (left panel) and $\zeta_e = 0.1$ (right panel).

Although there are apparent differences in particle spectra for different ζ_e, all our runs display clearly SHS behavior of the spectra of accelerated particles. The origin of this spectral evolution is easy to understand within the proposed model. The initial phase of the acceleration occurs in the linear regime (the test-particle approximation is still valid on this stage), which results in effective particle acceleration by the longitudinal large-scale turbulent motions and spectral hardening. However, fast particles accumulate a considerable fraction of the turbulent energy at this stage and start to exhaust the turbulence, so the efficiency of the acceleration decreases, which first affects higher-energy particles, resulting in spectrum softening.

Another important point, which can be noticed from the figure, is that the slope of the spectrum at the late decay phase (red solid curves) depends strongly on the injection efficiency ζ_e. In fact, the spectrum is much steeper in the case of strong injection. In practice, the spectrum in the right panel is so steep that it is probably undistinguishable against the background

thermal particle distribution. This means that the sequence of the (dash-dotted) spectra of accelerated electrons in the right panel will reveal itself as SHH evolution of the HXR spectrum. This conclusion is consistent with the fact that the SHH evolution is observed in stronger events, where enhanced injection of the charged particles (e.g., protons) is likely, and with a recent finding of gradual transitions between SHS and SHH evolution fragments (Grigis & Benz 2008), which requires a common acceleration mechanism for both SHS and SHH evolution patterns, even though additional spectral hardening in the gamma-ray range can occur due to relativistic particle trapping in the coronal loops (Krucker et al. 2008).

Besides the general SHS evolution, we should note that in agreement with previous studies of the stochastic acceleration (Miller et al. 1997; Grigis & Benz 2006) the spectra do not obey power laws exactly: breakup and breakdown turning points are evident from the plots. It should be noted here that since nonlinear effects were taken into account in the model the distribution function calculated for monoenergetic injection will not have any of the general properties of the Green function of a linear system. Therefore, one can no longer build the distribution function in the nonlinear case using the superposition principle. Nevertheless, the initial stage of the particle acceleration occurs in the linear regime if the loading parameter ζ_e is smaller than unity. Thus, broadly speaking, the general behavior of particle spectra evolution as illustrated in Figure 1 will hold for other relatively narrow (such as the first blue curves in Figure 1) initial particle distributions with a similar loading parameter defined by Equation (6).

Grigis & Benz (2006) demonstrated that the HXR spectra from the thin-target coronal sources are most directly linked to the energy spectra of the accelerated electrons, while the properties of the thick-target footpoint sources can essentially be affected by the transport effects. Accordingly, we computed the evolution of the thin-target HXR emission generated by the evolving ensemble of the accelerated electrons (as in Figure 1) and then derived the evolution of the HXR spectral index at $E = 35$ keV to compare with the observations of the coronal HXR sources reported by Battaglia & Benz (2006). The theoretical dependences of the HXR spectral index on time are shown in Figure 2 by three curves with different ratios of the acceleration time to the escape time. The asterisks in the plot show the evolution of the HXR spectral index observed for the coronal source in the 2002 December 4 event (Battaglia & Benz 2006). Even though no theoretical curve is an exact fit to the data, one can clearly note important similarities between theoretical and observational curves including the main SHS behavior and some hardening at the later stage.

Since the spectral index analysis of the coronal source can, in principle, be biased by a much stronger footpoint contribution, a more reliable method of thin-target HXR analysis could be the study of the occulted X-ray flares. However, the thin-target HXR flux is typically weak from the occulted coronal sources, so systematic statistical study of the occulted flares reports only the spectral data around the peak time of the flare (Krucker & Lin 2008). In some cases, however, it is still possible to derive information on the spectral evolution of the occulted flares by integrating the signal during the rise, peak, and decay phases, respectively. An example of the corresponding spectral index evolution in an occulted 2002 September 6 flare is shown by three long horizontal dashes in Figure 2 (E. Kontar 2008, private communication). SHS evolution is evident in this instance as well.

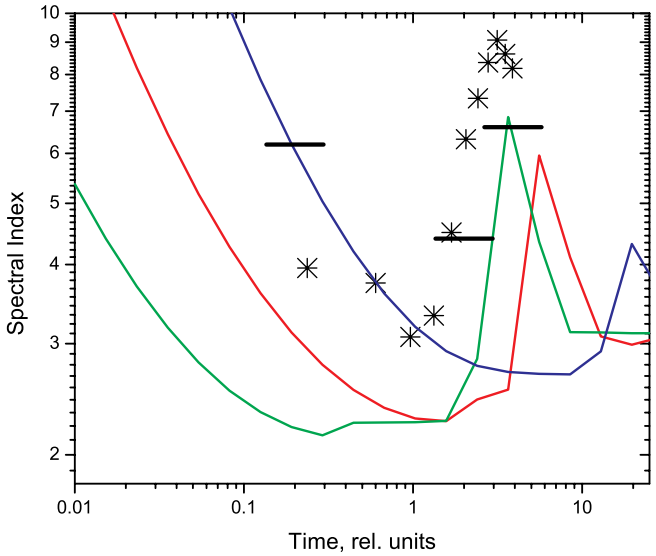

Figure 2. HXR spectral index evolution for theoretically calculated spectra with various ratios of the escape time to the acceleration time, $T_{esc}/\tau_{acc} = 5$ (solid curve), 1 (dashed curve), and 0.2 (dash-dotted curve); and observed from the 2002 December 4 flare, asterisks (Battaglia & Benz 2006), and from the occulted 2002 September 6 flare, horizontal dashes (E. Kontar 2008, private communication).

In addition to the aforementioned similarities between the theoretical and the observed spectra, there are also apparent differences. We have to note, however, that the differences between the theory and observations are less significant than the difference between the spectra observed from different events. Thus, we can ascribe these differences to the varying geometry of the source and/or to different regimes of the turbulence generation, cascading, damping, and escape, i.e., to those details of the model which have not been specifically addressed within this Letter.

To summarize, we note that taking into account the nonlinearity, which is necessarily present in a system where efficient acceleration by strong turbulence occurs, offers a plausible way of interpreting both kinds of the characteristic spectrum evolution, SHS and SHH, observed from solar flares. A side achievement of the model adopted here of the turbulent electron transport is the energy-independent escape time from the acceleration region, which implies that electrons with different energies leave the acceleration site simultaneously: a property required by measurements of the HXR fine structure timing (Aschwanden 2002). A full comprehensive picture of the particle acceleration in flares will require further analysis with shock waves, turbulence cascading, and injection details included, as well as computing the HXR and gamma-ray spectrum evolution, which we plan to consider elsewhere.

We are cordially grateful to Marina Battaglia for providing us with the data on the spectral index evolution from the coronal sources, and to Eduard Kontar, who obtained and provided us with the data on the spectral evolution of the occulted 2002 September 6 flare. The work was partly supported by Russian Foundation for Basic Research grants 06-02-16844, 06-02-16295, 08-02-92228, 09-02-00624 and by NSF grants AST-0607544 and ATM-0707319 to New Jersey Institute of Technology. We have made use of NASA's Astrophysics Data System Abstract Service.

REFERENCES

Abramenko, V. I. 2005, ApJ, 629, 1141
Akimov, V. V., et al. 1992, Sov. Astron. Lett., 18, 69
Anastasiadis, A., & Vlahos, L. 1991, A&A, 245, 271
Aschwanden, M. J. 2002, in Particle Acceleration and Kinematics in Solar Flares: A Synthesis of Recent Observations and Theoretical Concepts, ed. M. J. Aschwanden, & L. Martin Advanced Technology Center, Palo Alto, CA, USA (Dordrecht: Kluwer) (reprinted from Space Sci. Rev., 101)
Bastian, T. S., Fleishman, G. D., & Gary, D. E. 2007, ApJ, 666, 1256
Battaglia, M., & Benz, A. O. 2006, A&A, 456, 751
Benz, A. O. 1977, ApJ, 211, 270
Benz, A. O. 1986, Sol. Phys., 104, 99
Brown, J. C., Kontar, E. P., & Veronig, A. M. 2007, in Lecture Notes in Physics, Vol. 725, ed. K.-L. Klein & A. L. MacKinnon (Berlin: Springer), 65
Brown, J. C., & Loran, J. M. 1985, MNRAS, 212, 245
Bykov, A. M. 2001, Space Sci. Rev., 99, 317
Bykov, A. M., & Fleishman, G. D. 1992, MNRAS, 255, 269
Bykov, A. M., & Toptygin, I. N. 1990a, Zh. Eksp. Teor. Fiz., 97, 194
Bykov, A. M., & Toptygin, I. N. 1990b, Zh. Eksp. Teor. Fiz., 98, 1255
Bykov, A. M., & Toptygin, I. N. 1993, Phys.—Usp., 36, 1020
Cane, H. V., McGuire, R. E., & von Rosenvinge, T. T. 1986, ApJ, 301, 448
Cargill, P. J., Vlahos, L., Turkmani, R., Galsgaard, K., & Isliker, H. 2006, Space Sci. Rev., 124, 249
Chupp, E. L. 1990, ApJS, 73, 213
Cliver, E. W., Dennis, B. R., Kiplinger, A. L., Kane, S. R., Neidig, D. F., Sheeley, N. R., Jr., & Koomen, M. J. 1986, ApJ, 305, 920
Dennis, B. R., Hudson, H. S., & Krucker, S. 2007, in Lecture Notes in Physics, Vol. 725, ed. K.-L. Klein & A. L. MacKinnon (Berlin: Springer), 33
Fleishman, G. D., Fu, Q. J., Wang, M., Huang, G.-L., & Melnikov, V. F. 2002, Phys. Rev. Lett., 88, 251101
Fletcher, L., & Hudson, H. S. 2008, ApJ, 675, 1645
Frost, K. J., & Dennis, B. R. 1971, ApJ, 165, 655
Grigis, P. C., & Benz, A. O. 2004, A&A, 426, 1093
Grigis, P. C., & Benz, A. O. 2005, A&A, 434, 1173
Grigis, P. C., & Benz, A. O. 2006, A&A, 458, 641
Grigis, P. C., & Benz, A. O. 2008, ApJ, 683, 1180
Hamilton, R. J., & Petrosian, V. 1992, ApJ, 398, 350
Holman, G. D. 1985, ApJ, 293, 584
Holman, G. D., & Benka, S. G. 1992, ApJ, 400, L79
Hudson, H., & Vilmer, N. 2007, in Lecture Notes in Physics, Vol. 725, ed. K.-L. Klein & A. L. MacKinnon (Berlin: Springer), 81
Kane, S. R., & Anderson, K. A. 1970, ApJ, 162, 1003
Kiplinger, A. L. 1995, ApJ, 453, 973
Krucker, S., Hurford, G. J., MacKinnon, A. L., Shih, A. Y., & Lin, R. P. 2008, ApJ, 678, L63
Krucker, S., & Lin, R. P. 2008, ApJ, 673, 1181
Lin, R. P., & Schwartz, R. A. 1987, ApJ, 312, 462
Litvinenko, Y. E. 1996, ApJ, 462, 997
Litvinenko, Y. E. 2000, Sol. Phys., 194, 327
Litvinenko, Y. E. 2003, Adv. Space Res., 32, 2385
Mathews, T., & Venkatesan, D. 1990, Nature, 345, 600
Meyer, P., Parker, E. N., & Simpson, J. A. 1956, Phys. Rev., 104, 768
Miller, J. A. 1997, ApJ, 491, 939
Miller, J. A., Larosa, T. N., & Moore, R. L. 1996, ApJ, 461, 445
Miller, J. A., et al. 1997, J. Geophys. Res., 102, 14631
Nita, G. M., Gary, D. E., & Fleishman, G. D. 2005, ApJ, 629, L65
Park, B. T., Petrosian, V., & Schwartz, R. A. 1997, ApJ, 489, 358
Parks, G. K., & Winckler, J. R. 1969, ApJ, 155, L117
Petrosian, V., & Bykov, A. M. 2008, Space Sci. Rev., 134, 207
Petrosian, V., McTiernan, J. M., & Marschhauser, H. 1994, ApJ, 434, 747
Pryadko, J. M., & Petrosian, V. 1998, ApJ, 495, 377
Saldanha, R., Krucker, S., & Lin, R. P. 2008, ApJ, 673, 1169
Shibasaki, K. 2001, ApJ, 557, 326
Shibata, K. 1999, Ap&SS, 264, 129
Tsuneta, S. 1985, ApJ, 290, 353
Vlahos, L. 2007, in Lecture Notes in Physics, Vol. 725, ed. K.-L. Klein & A. L. MacKinnon (Berlin: Springer), 15
Yan, H., Lazarian, A., & Petrosian, V. 2008, ApJ, 684, 1461
Zaitsev, V. V., & Stepanov, A. V. 1992, Sol. Phys., 139, 343